Current Research in Bioinformatics

Research Article

Computational Validation of Selected Compounds from the GC-MS Profile of *Abies numidica* Essential Oil and their Antibacterial Effects

Abdelouahab Dehimat[1], Boudjellal Fayssal[2], Salem Dounya[3], Rouane Sarra[3] and Kharkhache Amina[3]

[1]*Department of Natural and Life Sciences, Faculty of Sciences, University of M'sila, University Pole, Road Bordj Bou Arreiridj, M'sila 28000, Algeria*
[2]*Department of Pharmacy, Laboratory of Investigation and Research Specialized in Health, Environment and Innovation of Pharmacy Faculty of Medicine, Setif 1 University Ferhat ABBAS Road, Setif 19137, Algeria*
[3]*Department of Microbiology and Biochemistry, University of M'sila, University Pole, Road Bordj Bou Arreiridj, M'sila 28000, Algeria*

Article history
Received: 29-05-2025
Revised: 18-08-2025
Accepted: 01-10-2025

Corresponding Author:
Abdelouahab Dehimat
Department of Natural and Life Sciences, Faculty of Sciences, University of M'sila, University Pole, Road Bordj Bou Arreiridj, M'sila 28000, Algeria
Email: a-ouahab.dehimat@univ-msila.dz

Abstract: This work examined the chemical composition of the Algerian endemic tree *Abies numidica* (Pinaceae) and investigated the antibacterial potential of three major constituents of its essential oil-Santene, Linalyl acetate, and 2,6-Octadiene-2,6-dimethyl-as reported in previously published GC-MS data. Computational antibacterial screening was carried out by docking the selected compounds onto the bacterial proteins 5Z9N (Staphylococcus aureus) and 3AQC (Micrococcus luteus). Molecular docking demonstrated that the active compounds of the EO, including 2,6-Octadiene, 2,6-dimethyl (Cp3), Linalyl acetate (Cp2), and Santene (Cp1), interacted effectively with the active sites of bacterial proteins 5Z9N and 3AQC. Notably, Cp3 (2,6-Octadiene, 2,6-dimethyl) demonstrated the best overall affinity, outperforming both the native ligands and reference molecules with the binding energies for Cp3 (2,6-Octadiene, 2,6-dimethyl) were-4.8 kcal/mol (5Z9N) and-4.1 kcal/mol (3AQC), indicating stronger interactions. These compounds formed critical bonds with amino acids such as Ile78, Val71, and Ala47 (5Z9N) and Val76, Leu116, and Ala79 (3AQC), suggesting their role in disrupting bacterial function. Furthermore, ADMET and BOILED-Egg analyses further showed favorable drug-likeness, with all compounds meeting Lipinski's criteria, exhibiting logP values below 4, and demonstrating suitable absorption and P-glycoprotein interaction profiles. Based on these results, we refer the antibacterial activity of the EO of *Abies numidica,* against the *M. luteus* and *S. aureus,* is suggesting to the presence of these compounds.

Keywords: *Abies numidica*, Essential Oil, Antibacterial Activity, In-Silico, 5Z9N, 3AQC

Introduction

The overuse of antibiotics has accelerated the rise of multi-resistant bacterial strains, presenting a continuously evolving global health challenge with potentially severe consequences. Since their discovery, antibiotics have been our primary defence mechanism. However, with the emergence of resistance, they risk becoming ineffective, potentially returning society to pre-antibiotic conditions (Pulcini *et al.,* 2019). Thus, antibiotic resistance among pathogens poses a significant public health issue (Zmantar *et al.,* 2008).

Finding natural molecules with antimicrobial properties is also critically important in the medical field. Essential oils may serve as a promising reservoir of bioactive compounds with antimicrobial properties. They contain a variety of secondary metabolites that can inhibit or slow bacterial growth. Essential oils and their components work through mechanisms targeting different pathways. The antimicrobial effects of various types of

aromatic plants and spices have long been recognized and empirically utilized (Lograda *et al.,* 2010).

Known for its natural resources, Algeria has a unique, rich, and diverse flora. Among its medicinal plants is *Abies numidica* (Gaussen and Leroy, 1982). This species belongs to a natural heritage area of high cultural value. This member of the Abietaceae family is listed among Rare and threatened plants but remains understudied despite its forest and aesthetic importance and the various biological activities of its secondary metabolites (Naili, 2016).

Computational methods in drug discovery play a crucial role in identifying potential drug candidates from vast compound libraries (Mak *et al.,* 2023). The integration of both structure-based and ligand-based approaches not only optimises the process but also enhances accuracy. This combined strategy is promising, particularly in identifying natural product-based compounds (Jana *et al.,* 2018). This method aims to determine the optimal binding mode of the "ligand-receptor" complex and predict the so-called "bioactive" conformation of the ligand within the receptor (Bouaziz-Terrachet, 2006; Pearson, 2008).

Previous studies have reported the GC-MS phytochemical profile of *Abies numidica* Essential Oil (EO) and its in vitro antibacterial activity (Benouchenne *et al*., 2020). Building on these findings, we hypothesized that only a subset of the identified compounds would exhibit strong binding affinities toward bacterial targets 5Z9N (Staphylococcus aureus) and 3AQC (Micrococcus luteus). Such interactions could partially explain the experimentally observed antibacterial activity. To investigate this, we conducted an in silico study, selecting three major compounds from the reported GC-MS profile Santene, Linalyl acetate, and 2,6-Octadiene-2,6-dimethyl and evaluated their binding to the two bacterial protein targets using molecular docking, aiming to identify potential bioactive molecules responsible for the observed effects.

Materials and Methods

Preparation of Structures

Ligand Structure

The 3D structure of the ligand used in this study was imported in SDF format from the PubChem database. After selecting the downloaded ligand, energy optimization was performed. The 3D structures of these ligands were then prepared and saved in Mol2 format using the Avogadro software (Table 1).

Table 1: Tested Ligands Structures

Number	Compounds Names	%	Formulate	ID	Structures
Cp1	Santene	0.23	C9H14	10720	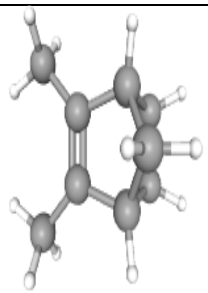
Cp2	Linalyl acetate	7.42	C12H20O2	8294	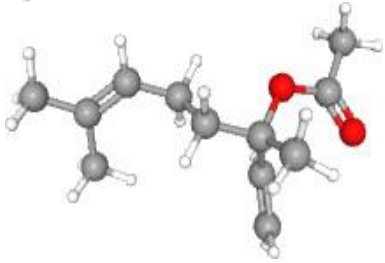
Cp3	2,6-Octadiene, 2,6-dimethyl	7.63	C10H18	5365898	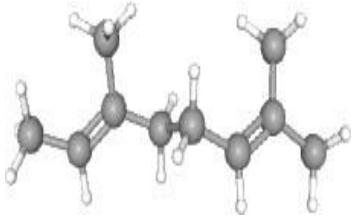

DOI: 10.3844/ajbsp.2025.1.9

Protein Structures

The selected protein structures in their complex states were retrieved from the RCSB database and downloaded in PDB format. Protein structures were cleaned by removing water molecules and ligands using BIOVIA Discovery Studio. Active binding sites of the target proteins were identified using the same software based on literature data. The complex involves the GyrB ATPase domain of *S. aureus* with the reference inhibitor 4,6-dichloro-2-(methylthio) pyrimidine. The selected structure (PDB ID: 5Z9N) is a chain dimer (A) with a resolution of 2.54 Å. This protein is known to inhibit phagocytosis and to help the bacteria evade the immune system (Figure 1).

For *M. lutus*, the complex involves B-P 26 heterodimeric hexaprenyl diphosphate synthase with magnesium and an FPP analogue. The selected 3D structure (PDB ID: 3AQC) is a chain dimer (B, D) with a resolution of 2.61 Å. Combines with enzymes and inhibits phagocytosis (Figure 2).

The reference inhibitors for each target proteins were cited in Table 2.

Table 2: Complexes Selected for Docking Studies

Protein Strains (Downloaded from PDB Database)		
	S. aureus	*M. luteus*
Complex (PDB ID)	5Z9N	3AQC
Reference Ligand (Re-Docked)	4,6-dichloro-2-(methylthio)pyrimidine	FPP analogue (Photo-affinity of farnesyl pyrophosphate)
Active Site Residues (Amino Acids)	Val71, Ala47, Glu50, Ile78, Asn46, Val120	Val142, Leu116, His83, Ala79, Val76, Lys225, Arg93, Lys170

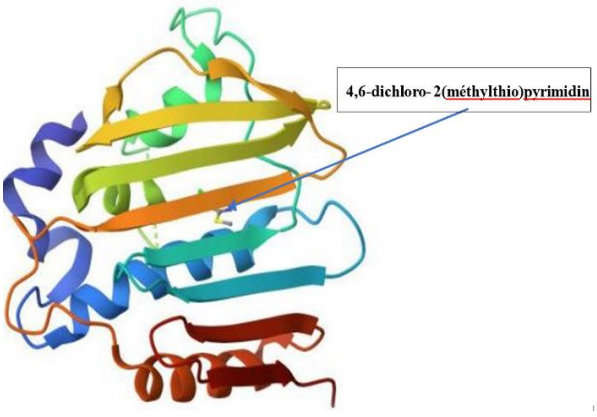

Fig. 1: 3D Structure of 5Z9N Complexed with Its Standard Inhibitor (GyrB ATPase)

Fig. 2: 3D Structure of 3AQC Complexed with Its Standard Inhibitor

Computational Modelling Using Molecular Docking

Auto dock Vina is a program that simulates and evaluates how a small molecule binds to a protein. It helps to find potential drugs from large collections of chemicals. The ligands (Santene, Linalyl acetate and 2,6-Octadiene-2,6-dimethyl) and target protein (5Z9N and 3AQC) files, typically in formats like PDB or MOL2, were prepared. Specific input parameters, including grid size, exhaustiveness, and scoring function options, were set to control the docking process. Auto dock Vina generated a grid map based on the specified grid size, defining the search space within the receptor for ligand binding evaluation. This software explores various ligand conformations and orientations within the receptor's binding site to calculate binding affinities. A scoring function estimates the strength of ligand-receptor interactions. Upon completion, Auto dock Vina provided output files containing information about predicted ligand binding poses and their docked scores. Docking will be analyzed by the results to identify favorable ligand binding modes and evaluate binding affinities (Fährrolfes *et al.,* 2017).

ADME-Toxicity Prediction

Following the molecular docking screening, the selected compounds were analyzed by ADME/Tox studies and Physio-Chemically profiled. Drug toxicity had been predicted by using SWISSADME. Swiss ADME was developed to meet the needs of drug discovery and medicinal chemistry fields, where a crucial emphasis is placed on maintaining a balance between accuracy and speed to handle a substantial volume of molecules (Daina *et al.,* 2017).

Results

The antibacterial activity and a phytochemical analysis using GC-MS identified 29 compounds in the EO profile of the Essential Oil (EO) from *A. numidica,* obtained in the Constantine region (eastern Algeria), was evaluated (Benouchenne *et al.,* 2020). Among these, three selected compounds were further assessed

DOI: 10.3844/ajbsp.2025.1.9

in silico using molecular docking to evaluate their interactions with target proteins from sensitive bacterial strains.

Re-docked Reference Ligands (Validation of Molecular Docking With Reference Ligands)

The re-docking results confirmed that the standard inhibitors, 4,6-dichloro-2-(methylthio) pyrimidine and the FPP analogue, aligned with literature data. They demonstrated similar orientations within the active site pockets of 5Z9N (Val71, Ala47, Glu50, Ile78, Asn46, Val120) and 3AQC (Val142, Leu116, His83, Ala79, Val76, Lys225, Arg93, Lys170), respectively (Figure 3).

Table 3: Key Binding Affinities of Isolated Compounds with Selected Receptors

Receptor	*S. aureus (5Z9N)*	*M. luteus (3AQC)*
Compound	Binding Energy (kcal/mol)	Binding Energy (kcal/mol)
Reference	-3.8	-5.4
Cp1: Santene	-4.8	-4.1
Cp2: Linalyl acetate	-5.2	-4.5
Cp3: 2,6-octadiene, 2,6-dimethyl	-5.3	-4.7

Binding Affinities of the Elucidated Compounds With the Selected Receptors

Molecular docking calculations yielded several conformations with varying energy values for the protein-ligand complexes. The conformation with the lowest binding energy indicates the preferred ligand arrangement within the receptor, as shown in Table 3.

The compounds were ranked in ascending order, with those showing more negative binding energy values demonstrating better receptor affinity:

- 5Z9N: 2,6-Octadiene, 2,6-dimethyl < Linalyl acetate < Santene < Reference
- 3AQC: Reference < 2,6-Octadiene, 2,6-dimethyl < Linalyl acetate < Santene

Interactions Among the Compounds With 5Z9N

The binding mode of Linalyl acetate revealed three alkyl interactions with Val71, Ala47, and Ile78. Additionally, three Van Der Waals (VDW) interactions were observed with Asp73, Thr165, and Val167. In addition, Santene formed one alkyl bond with Ile78, while 2,6-Octadiene, 2,6-dimethyl formed alkyl interactions with Ile78, Val71, and Ala47, correspondingly (Figure 4).

The results indicate that Santene, Linalyl acetate, and 2,6-Octadiene, 2,6-dimethyl may have inhibitory effects on the 5Z9N receptor by forming key bonds with amino acids within the pocket. Compared to the standard inhibitor of 5Z9N (4,6-dichloro-2-(methylthio)pyrimidine), the docking study revealed acceptable alignment for all docked compounds, except Linalyl acetate. The three active compounds interact with the critical amino acid residues of the protein's active site, contributing to inhibitory activity against 5Z9N. Among them, 2,6-Octadiene, 2,6-dimethyl demonstrated the highest affinity with the lowest binding energy (-5.3 kcal/mol) compared to the native ligand (-3.8 kcal/mol) (Figure 5).

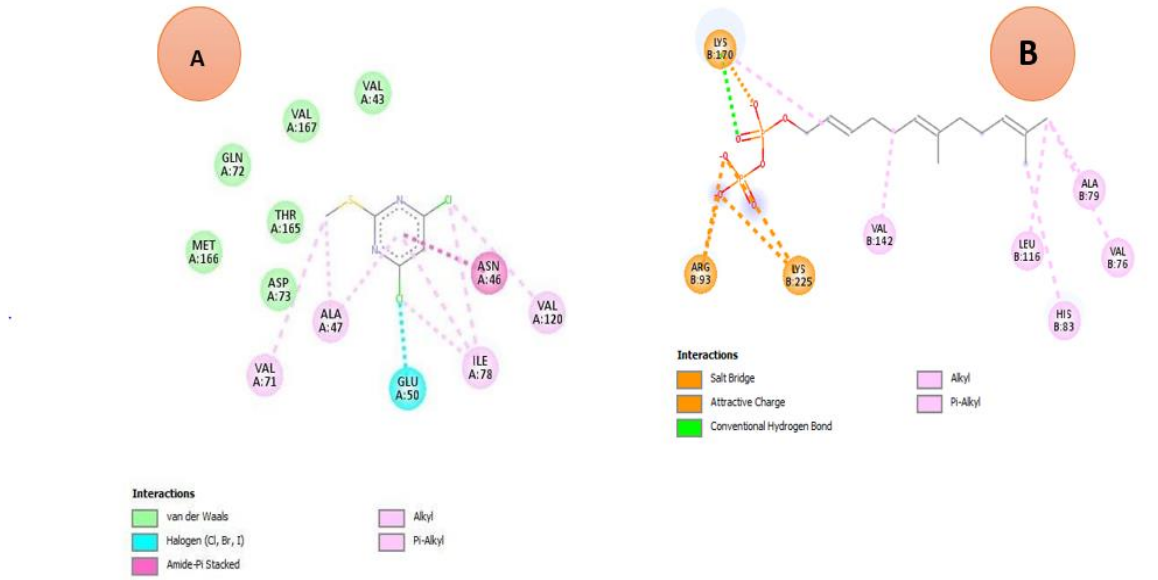

Fig. 3: 2D Views of Binding Positions for 4,6-dichloro-2-(methylthio) pyrimidine in 5Z9N (A) and FPP Analogue in 3AQC (B)

DOI: 10.3844/ajbsp.2025.1.9

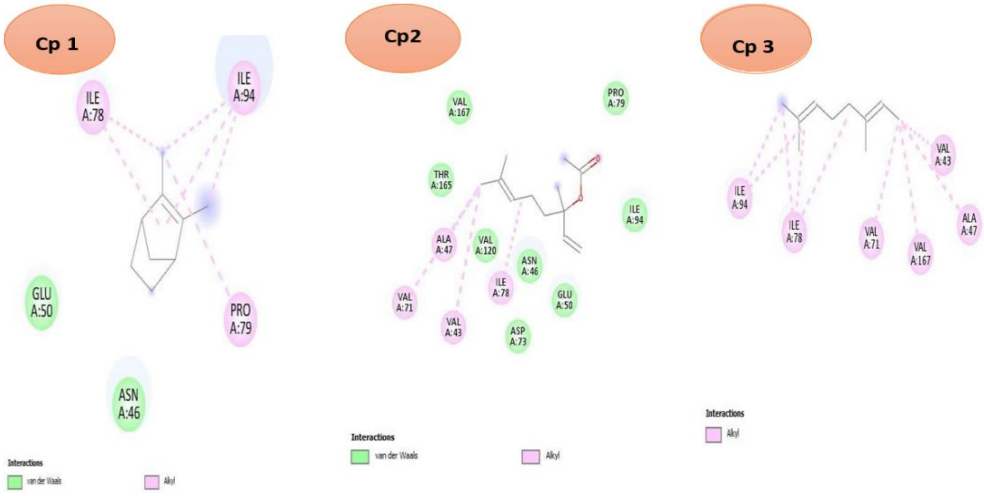

Fig. 4: 2D View of the Binding Positions of Cp1 (Santene), Cp2 (Linalyl acetate), and Cp3 (2,6-Octadiene, 2,6-dimethyl) in Protein 5Z9N

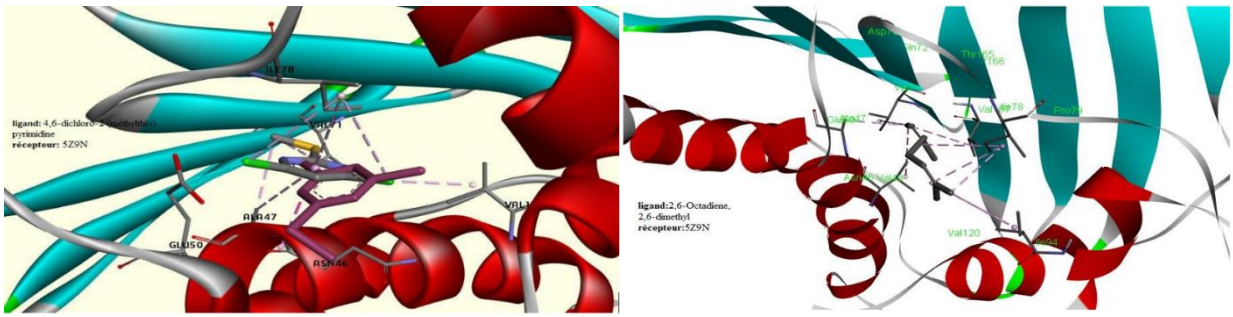

Fig 5: 3D Alignment of Cp3 (2,6-Octadiene, 2,6-dimethyl) Within the 5Z9N Pocket Compared to the Reference Ligand

Interactions Among the Compounds With 3AQC

Linalyl acetate formed three alkyl interactions with Val76, Leu116, and Ala79, along with one Pi-sigma interaction with His83. Santene interacted with Leu116, Ala79, Val76, and also exhibited a Pi-sigma interaction with His83. Similarly, 2,6-Octadiene, 2,6-dimethyl displayed alkyl interactions with Val76, Val142, Ala79, and Leu116, along with a Pi-sigma interaction with His83 (Figure 6).

The docking study revealed that these compounds form multiple associations with key amino acids in the protein pocket, suggesting inhibitory potential against 3AQC. Based on the binding energies shown in Table 3, all docked compounds exhibited higher affinity for the binding site of 3AQC compared to the native ligand (FPP analogue). The 2D interaction diagram revealed acceptable alignment for all compounds, except 2,6-Octadiene, 2,6-dimethyl. This supports the bioactivity of the docked compounds against 3AQC. Among the active compounds tested, 2,6-Octadiene, 2,6-dimethyl demonstrated the strongest inhibitory profile, with a binding energy of-4.7 kcal/mol. This was followed by Linalyl acetate (-4.5 kcal/mol) and Santene (-4.1 kcal/mol) (Figure 7). When compared to the reference ligand FPP (Farnesyl Pyrophosphate), which interacts with amino acids in the active site of 3ACQ namely Val142, Leu116, His83, Ala79, Val76, Lys225, Arg93, and Lys170—2,6-Octadiene, 2,6-dimethyl exhibited distinct interaction patterns. It formed interactions with Val76, Val142, Cys143, Ile139, Ala79, Leu116, His113, His83, Ser80, and Gly112, highlighting its potential as a promising antibacterial agent (Figure 7).

Toxicity Prediction of the Drug Candidates

The selected compounds were further analyzed for the ADME-T analysis. Santene, Linalyl acetate and 2,6-Octadiene-2,6-dimethyl were analyzed by SWISSADME. Best ADMET properties lie in the category where the log p-value is less than 4 and more soluble. Borneol showed the best ADMET properties and it did not violate any Lipinski's rule and its log p value was less than 4 with more solubility (Tables 4).

DOI: 10.3844/ajbsp.2025.1.9

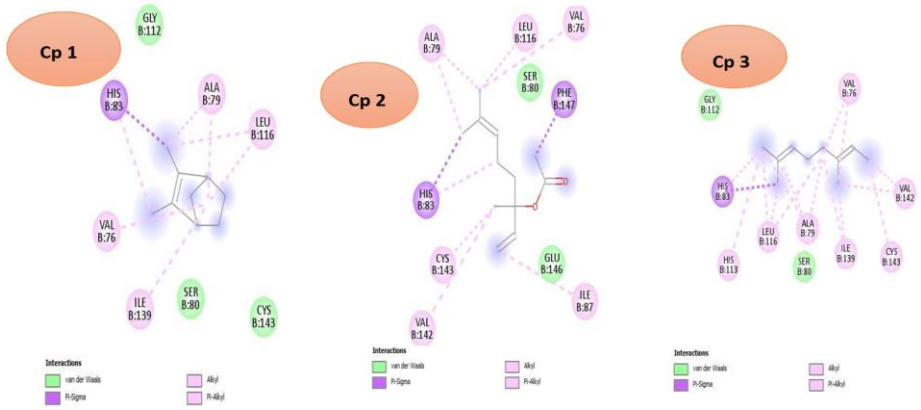

Fig. 6: 2D View of the Binding Positions of Cp1 (Santene), Cp2 (Linalyl acetate), and Cp3 (2,6-Octadiene, 2,6-dimethyl) in Protein 3AQC

Table 4: ADME-T and Drug-Likeness Properties of Selected Compounds

ENTRY	TPSA	#ROTATABLE BONDS	MW G/MOL	WLOGP	MLOGP	#H-BOND ACCEPTORS	#H-BOND DONORS	VEBER #VIOLATIONS	LIPINSKI #VIOLATIONS	GHOSE #VIOLATIONS	BIOAVAILABILITY SCORE
RANGE	<140	<11				<10	<5	<= 1	<=1	<=1	
Cp 1	26.3	6	196.29	3.24	2.95	2	0	0	0	0	0.55
Cp 2	0	3	138.25	3.7	3.66	0	0	0	0	1	0.55
Cp 3	0	0	122.21	2.75	3.98	0	0	0	0	1	0.55
ADME-T	Absorption	Distribution	Metabolism				Excretion	Toxicity			
	GI absorption	BBB permeant	CYP1A2 inhibitor	CYP2C19 inhibitor	CYP2C9 inhibitor	CYP2D6 inhibitor	CYP3A4 inhibitor	substrate	Total Clearance	AMES	Herg I/II Inhibitors
Cp 1	High	Yes	No	No	No	No	No	Yes	0	No	No
Cp 2	Low	Yes	No	No	No	No	No	Yes	0	No	No
Cp 3	Low	Yes	No	No	No	No	No	Yes	0	No	No

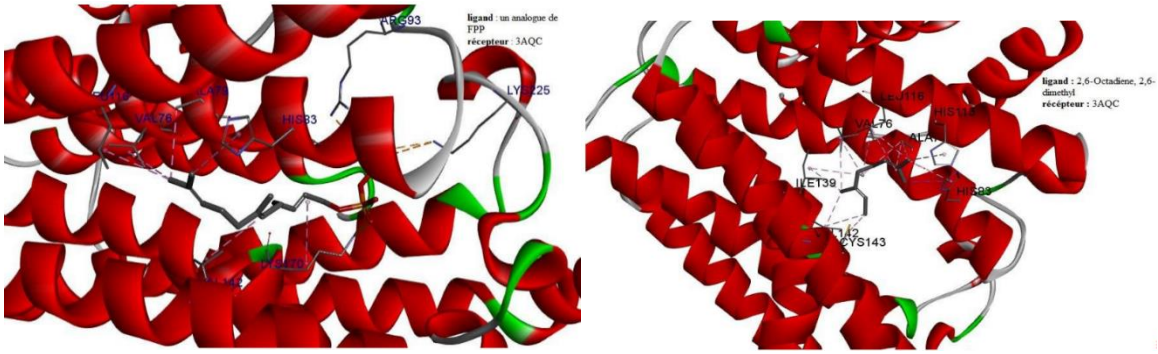

Fig. 7: 3D Alignment of Cp3 (2,6-Octadiene, 2,6-dimethyl) Inside the 3AQC Pocket Compared to the Reference Ligand

Boiled egg analysis from ADME suggested that if a compound has P-glycoprotein (PGP)-value, it shows that it has a strong bond with P-glycoprotein (PGP) and the drug will target the site after crossing the membrane. In the graphical representation, blue dots indicate molecules that are predicted to be expelled from the central nervous system via P-glycoprotein, whereas red dots represent molecules predicted to remain within the central nervous system without being expelled through P-glycoprotein.

In the provided visualization, the egg yolk points symbolize molecules that have the potential to passively traverse the Blood-Brain Barrier, while the egg white points represent molecules that may passively cross the gastrointestinal tract. The blue and red dots on the plot indicate molecules that are predicted to be expelled or retained by P-glycoprotein, singly shown in Figure 8.

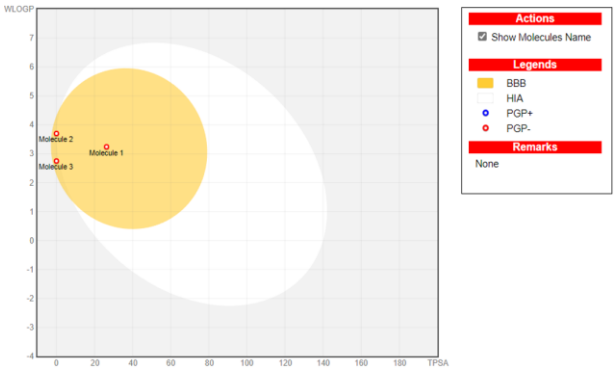

Fig. 8: Shows the boiled egg analysis by ADME

Discussion

The GC-MS profile of A. numidica EO used in this study was obtained from the work of Benouchenne *et al.* (2024). From this profile, six major compounds were initially considered for molecular docking analysis against bacterial protein targets. Based on binding energy results, only the three compounds demonstrating the most significant affinities were analyzed and discussed in detail.

The essential oil (EO) of *A. numidica* showed a slight antibacterial capacity, predominantly against *S. aureus*, with β-Caryophyllene and α-pinene identified as major compounds responsible for the observed antimicrobial activity (Dahham *et al.*, 2015).

These findings are consistent with studies on other species, such as *A. cilicia*, where resin extracts were reported to effectively inhibit microbial growth (Kizil *et al.*, 2002). This suggests that the antimicrobial efficacy of species may be attributed to specific bioactive compounds like terpenes. Interestingly, The EO of Algerian A. numidica, collected in Seraidi, Annaba, showed significant antimicrobial effects against Gram-negative bacteria such as E. coli. However, it exhibited only mild inhibitory effects on the Gram-positive S. aureus (Ramdani *et al.*, 2021).

This contrasts with the EO from white fir (*Abies alba*), which exhibited no effect on various bacterial strains except for *S. aureus* (Yang *et al.*, 2009). The selective activity against *S. aureus* in these studies could be linked to differences in chemical composition, as β-Caryophyllene, a major compound in *A. numidica*, is known for its potent antimicrobial properties. Further comparisons reveal that EO from needles of *A. numidica*, collected in Babors, Algeria, exhibited strong activity against both *S. aureus* and *M. luteus* (Ghadbane *et al.*, 2016).

This aligns with the findings of Bellil and Benouchenne *et al.* (2024), who also identified β-Caryophyllene as a dominant compound but noted that the EO had no effect on most tested bacterial strains apart from *S. aureus*. Such variations highlight the influence of environmental factors, plant part, and harvesting conditions on the antimicrobial properties of EOs. The diterpene abietanes isolated from the cones of *A. numidica* also displayed significant antimicrobial properties (Belhadj Mostefa *et al.*, 2017). These compounds, although distinct from β-Caryophyllene and α-pinene, further support the potential of A. numidica as a source of diverse bioactive molecules with antimicrobial activity.

On the other hand, the toxicity analysis of the drug candidate is mandatory as it analyzes the lipophilicity, toxicity and solubility of the active compound (Coutanceau *et al.*, 2005). The ADMET analysis of the selected predicted compounds was performed and results showed that borneol exhibits good ADMET properties while Cp1 is highly soluble regarding to the Cp2 and Cp3 which is poorly soluble. The lipophilicity iLogP value of three selected compounds is less than 5 which means that it does follow the five rule of Lipinski's which is that The molecular weight should not exceed 500 Da, with no more than 10 hydrogen bond acceptors and 5 hydrogen bond donors (Bakchi *et al.*, 2022).

The current study shows that drug candidates derived from medicinal plant Cp 1 have a high binding affinity with high GI absorption and it does cross the Blood-Brain Barrier (BBB). These characteristics of borneol position it as a highly promising and soluble drug candidate. The EGG-boiled analysis shows that the molecule may cross the blood-brain barrier and gastrointestinal tract as shown in Figure 8. Hydrogels are widely employed in wound healing applications due to their excellent capacity to retain water. However, these hydrogels could be easily applied and removed without affecting the wound but have poor water-soluble drug delivery systems due to their intrinsic hydrophobic nature (Hall *et al.*, 2022; Naveed *et al.*, 2025).

Conclusion

This in silico investigation of the antibacterial activity of A. numidica Essential Oil (EO) revealed important inhibitory potential against S. aureus and M. luteus. The molecular docking results demonstrated that the EO's active compounds, including Santene (Cp1), Linalyl acetate (Cp2), and 2,6-Octadiene, 2,6-dimethyl (Cp3), interacted effectively with the active sites of

bacterial proteins 5Z9N and 3AQC. Notably, Cp3 (2,6-Octadiene, 2,6-dimethyl) demonstrated the best overall affinity, outperforming both the native ligands and reference molecules. The results highlight the unique potential of A. numidica EO as a natural source of antibacterial agents, particularly due to the activity of its bioactive components emphasizing their relevance in addressing the growing challenge of antibiotic resistance. In addition, the ADMET analysis of the selected compounds was performed and results showed that all compounds exhibited favorable ADMET properties. Future studies, including in vitro and in vivo validation, and eventually clinical trials, will be necessary to confirm the therapeutic potential of A. numidica EO-derived compounds against multidrug-resistant pathogens.

Limitations

This study was limited to a computational approach, using molecular docking and ADMET predictions based on the published GC-MS profile of A. numidica EO. No new antibacterial assays were conducted, and the results require experimental validation. Only the three compounds with the highest predicted affinities were analyzed, and ADMET predictions remain theoretical until tested in vitro or in vivo. Nevertheless, as the first in silico investigation of A. numidica EO, this work provides a solid foundation for future experimental and translational studies.

Acknowledgment

I sincerely thank Benramdhan Zeynab for her involvement in the project and for validating the molecular docking protocol.

Funding Information

The authors have not received any financial support or funding to report.

Authors Contributions

Abdelouahab Dehimat: Participated in experiments, coordinated data analysis, and contributed to manuscript preparation. Designed the research plan and organized the study. Contributed to the conception, design, acquisition, and interpretation of data. Contributed to drafting or critically reviewing the article for intellectual content and provided final approval for submission and revisions.

Boudjellal Fayssal: Give final approval of the version to be submitted and any revised version.

Salem Dounya, Rouane Sarra and Kharkhache Amina: Run the protocol and contributed to the writing of the manuscript.

Ethics

This study was performed entirely using a computational approach. No new plant material was collected, and no new in vitro or in vivo experiments were conducted.

References

Bakchi, B., Krishna, A. D., Sreecharan, E., Ganesh, V. B. J., Niharika, M., Maharshi, S., Puttagunta, S. B., Sigalapalli, D. K., Bhandare, R. R., & Shaik, A. B. (2022). An overview on applications of Swiss ADME web tool in the design and development of anticancer, antitubercular and antimicrobial agents: A medicinal chemist's perspective. *Journal of Molecular Structure*, *1259*, 132712. https://doi.org/10.1016/j.molstruc.2022.132712

Belhadj Mostefa, M., Abedini, A., Voutquenne-Nazabadioko, L., Gangloff, S. C., Kabouche, A., & Kabouche, Z. (2017). Abietane diterpenes from the cones of *Abies numidica* de Lannoy ex Carrière (Pinaceae) and *in vitro* evaluation of their antimicrobial properties. *Natural Product Research*, *31*(5), 568–571. https://doi.org/10.1080/14786419.2016.1190723

Benouchenne, D., Bellil, I., Akkal, S., Bensouici, C., & Khelifi, D. (2020). LC–MS/MS analysis, antioxidant and antibacterial activities of Algerian fir (*Abies numidica* de LANNOY ex CARRIÈRE) ethylacetate fraction extracted from needles. *Jordan Journal of Biological Sciences*, *32*(8), 3321–3327. https://doi.org/https://doi.org/10.54319/jjbs/150219

Bouaziz-Terrachet, S. (2006). *Conception d'inhibiteurs sélectifs de l'activité enzymatique de la cyclooxygénase-2*.

Benouchenne, D., Bellil, I., Bendjedid, S., Ramos, A., Nieto, G., Akkal, S., & Khelifi, D. (2024). The First Records of the In Silico Antiviral and Antibacterial Actions of Molecules Detected in Extracts of Algerian Fir (*Abies numidica* De Lannoy) Using LC-MS/MS Analysis. *Plants*, *13*(9), 1246. https://doi.org/10.3390/plants13091246

Coutanceau, E., Marsollier, L., Brosch, R., Perret, E., Goossens, P., Tanguy, M., Cole, S. T., Small, P. L. C., & Demangel, C. (2005). Modulation of the host immune response by a transient intracellular stage of Mycobacterium ulcerans: the contribution of endogenous mycolactone toxin. *Cellular Microbiology*, *7*(8), 1187–1196. https://doi.org/10.1111/j.1462-5822.2005.00546.x

Dahham, S., Tabana, Y., Iqbal, M., Ahamed, M., Ezzat, M., Majid, A., & Majid, A. (2015). The Anticancer, Antioxidant and Antimicrobial Properties of the Sesquiterpene β-Caryophyllene from the Essential Oil of Aquilaria crassna. *Molecules*, *20*(7), 11808–11829. https://doi.org/10.3390/molecules200711808

Daina, A., Michielin, O., & Zoete, V. (2017). SwissADME: a free web tool to evaluate pharmacokinetics, drug-likeness and medicinal chemistry friendliness of small molecules. *Scientific Reports*, *7*(1). https://doi.org/10.1038/srep42717

Fährrolfes, R., Bietz, S., Flachsenberg, F., Meyder, A., Nittinger, E., Otto, T., Volkamer, A., & Rarey, M. (2017). ProteinsPlus: a web portal for structure analysis of macromolecules. *Nucleic Acids Research*, *45*(W1), W337–W343. https://doi.org/10.1093/nar/gkx333

Gaussen, H., & Leroy, H. F. (1982). *Précis de botanique, végétaux supérieurs. Masson*.

Ghadbane, M., Bounar, R., Khellaf, R., Medjekal, S., Belhadj, H., Benderradji, L., Smaili, T., & Harzallah, D. (2016). Antioxidant and antimicrobial activities of endemictree *Abies numidica* growing in babor mountains from Algeria. *Global Journal of Research and Medicinal Plants and Indigenous Medecine*, *5*(1), 19–28.

Hall, B. S., Hsieh, L. T.-H., Sacre, S., & Simmonds, R. E. (2022). The One That Got Away: How Macrophage-Derived IL-1β Escapes the Mycolactone-Dependent Sec61 Blockade in Buruli Ulcer. *Frontiers in Immunology*, *12*, 788146. https://doi.org/10.3389/fimmu.2021.788146

Jana, S., Ganeshpurkar, A., & Singh, S. K. (2018). Multiple 3D-QSAR modeling, e-pharmacophore, molecular docking, and *in vitro* study to explore novel AChE inhibitors. *RSC Advances*, *8*(69), 39477–39495. https://doi.org/10.1039/c8ra08198k

Kizil, M., Kizil, G., Yavuz, M., & Aytekin, Ç. (2002). Antimicrobial Activity of Resins Obtained from the Roots and Stems of Cedrus libani and Abies cilicia. *Applied Biochemistry and Microbiology*, *38*(2), 144–146. https://doi.org/10.1023/a:1014358532581

Lograda, T., Chaker, A. N., Chalchat, J. C., Ramdani, M., Silini, H., Figueredo, G., & Chalard, P. (2010). Chemical Composition and Antimicrobial Activity of Essential Oils of *Genista ulicina* and *G. vepres Natural Product Communications*, *5*(5). https://doi.org/10.1177/1934578x1000500532

Mak, K.-K., Wong, Y.-H., & Pichika, M. R. (2023). Artificial Intelligence in Drug Discovery and Development. *Drug Discovery and Evaluation: Safety and Pharmacokinetic Assays*, 1–38. https://doi.org/10.1007/978-3-030-73317-9_92-1

Ramdani, M., Lograda, T., Mohamadi, Y., Figueredo, G., & Chalard, P. (2021). Chemical composition and antimicrobial activity of Myrtus communis essential oils from Algeria. *Biodiversitas Journal of Biological Diversity*, *22*(2). https://doi.org/10.13057/biodiv/d220249

Naveed, M., Ali, I., Aziz, T., Saleem, A., Rajpoot, Z., Khaleel, S., Khan, A. A., Al-harbi, M., & Albekairi, T. H. (2025). Computational and GC-MS screening of bioactive compounds from Thymus Vulgaris targeting mycolactone protein associated with Buruli ulcer. *Scientific Reports*, *15*(1). https://doi.org/10.1038/s41598-024-83908-0

Naili, O., (2016). *Effet des extraits de Abies numidica de Lannoy sur la croissance et sur la microflore caecale et fécale des poussins de chair Mémoire Pour l'obtention du diplôme de Doctorat*.

Pearson, B. (2008). Pearson's Correlation Coefficient. *Encyclopedia of Public Health*, 1090–1091. https://doi.org/10.1007/978-1-4020-5614-7_2569

Pulcini, C., Clerc-Urmes, I., Attinsounon, C. A., Fougnot, S., & Thilly, N. (2019). Antibiotic resistance of Enterobacteriaceae causing urinary tract infections in elderly patients living in the community and in the nursing home: a retrospective observational study. *Journal of Antimicrobial Chemotherapy*, *74*(3), 775–781. https://doi.org/10.1093/jac/dky488

Yang, S.-A., Jeon, S.-K., Lee, E.-J., Im, N.-K., Jhee, K.-H., Lee, S.-P., & Lee, I.-S. (2009). Radical Scavenging Activity of the Essential Oil of Silver Fir (Abies alba). *Journal of Clinical Biochemistry and Nutrition*, *44*(3), 253–259. https://doi.org/10.3164/jcbn.08-240

Zmantar, T., Chaieb, K., Ben Abdallah, F., Ben Kahla-Nakbi, A., Ben Hassen, A., Mahdouani, K., & Bakhrouf, A. (2008). Multiplex PCR detection of the antibiotic resistance genes in Staphylococcus aureus strains isolated from auricular infections. *Folia Microbiologica*, *53*(4), 357–362. https://doi.org/10.1007/s12223-008-0055-5